

See discussions, stats, and author profiles for this publication at: <https://www.researchgate.net/publication/275643681>

# Diarylethene Self-Assembled Monolayers: Cocrystallization and Mixing-Induced Cooperativity Highlighted by Scanning Tunneling Microscopy at the Liquid/Solid Interface

ARTICLE *in* CHEMISTRY - A EUROPEAN JOURNAL · AUGUST 2015

Impact Factor: 5.73 · DOI: 10.1002/chem.201500804

---

READS

39

## 6 AUTHORS, INCLUDING:



Denis Frath

Paris Diderot University

20 PUBLICATIONS 283 CITATIONS

[SEE PROFILE](#)



Kenji Matsuda

Hitachi, Ltd.

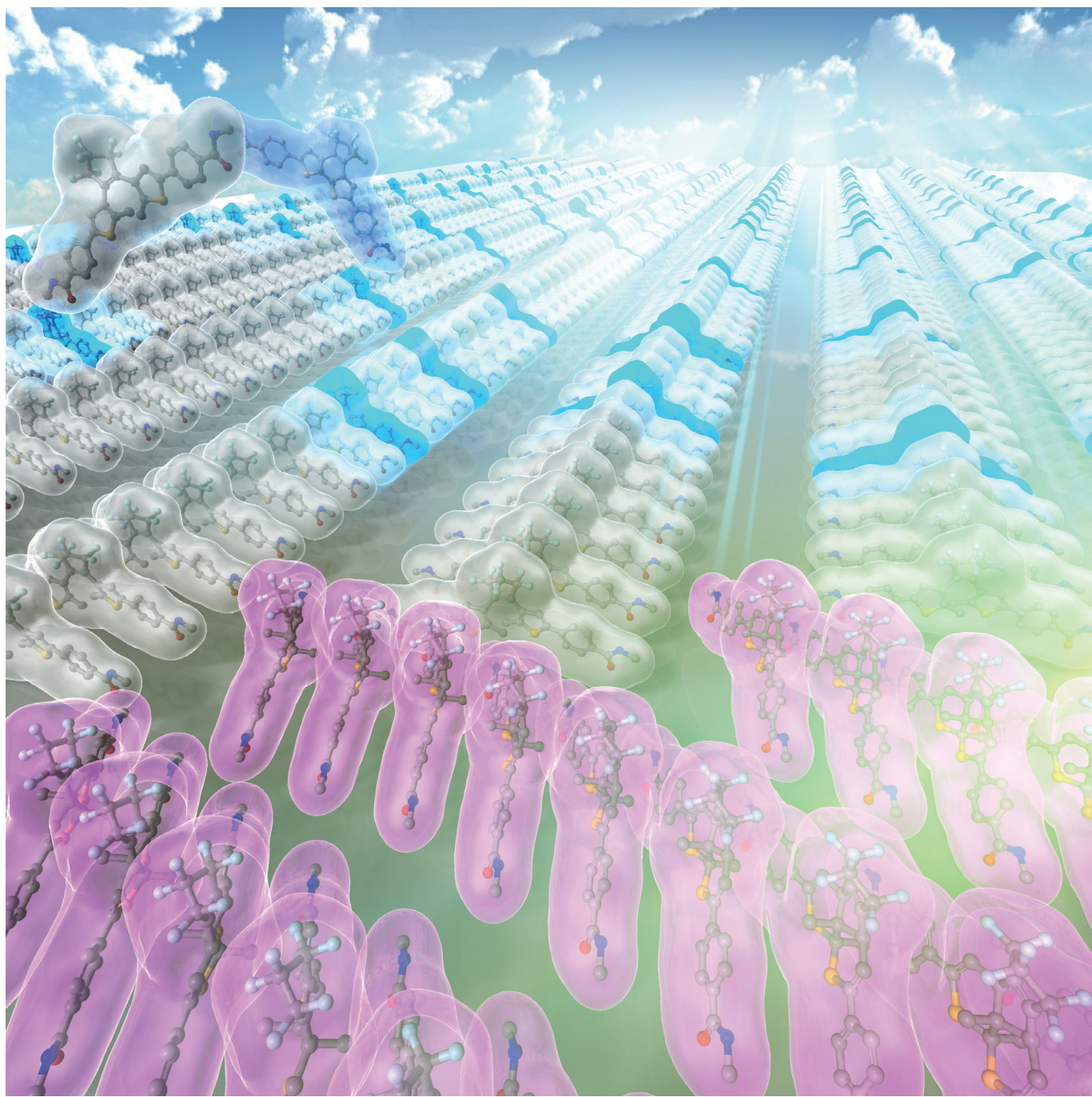
113 PUBLICATIONS 3,319 CITATIONS

[SEE PROFILE](#)

## ■ Cooperative Effects

# Diarylethene Self-Assembled Monolayers: Cocrystallization and Mixing-Induced Cooperativity Highlighted by Scanning Tunneling Microscopy at the Liquid/Solid Interface

Denis Frath, Takeshi Sakano, Yohei Imaizumi, Soichi Yokoyama, Takashi Hirose, and Kenji Matsuda\*<sup>[a]</sup>



**Abstract:** Stimulus control over 2D multicomponent molecular ordering on surfaces is a key technique for realizing advanced materials with stimuli-responsive surface properties. The formation of 2D molecular ordering along with photoisomerization was monitored by scanning tunneling microscopy at the octanoic acid/highly oriented pyrolytic graphite interface for a synthesized amide-containing diarylethene, which underwent photoisomerization between the open- and closed-ring isomers and also a side-reaction to give the annulated isomer. The nucleation ( $K_n$ ) and elongation ( $K_e$ ) equilibrium constants were determined by analysis of the

concentration dependence of the surface coverage by using a cooperative model at the liquid/solid interface. It was found that the annulated isomer has a very large equilibrium constant, which explains the predominantly observed ordering of the annulated isomer. It was also found that the presence of the closed-ring isomer induces cooperativity into the formation of molecular ordering composed of the open-ring isomer. A quantitative analysis of the formation of ordering by using the cooperative model has provided a new view of the formation of 2D multicomponent molecular ordering.

## Introduction

Control over molecular nanostructures has become of the upmost importance in the bottom-up strategy to elaborate functionalized surfaces for electronic devices.<sup>[1]</sup> In this context, the study of surface-confined self-assemblies of organic building blocks on surfaces such as Au(111) or highly oriented pyrolytic graphite (HOPG) has been the subject of intense research.<sup>[2–16]</sup> Two-dimensional (2D) supramolecular self-assembly can be efficiently characterized by scanning tunneling microscopy (STM) at the liquid/solid interface with single-molecule resolution,<sup>[17]</sup> which reveals influences of various factors such as concentration,<sup>[18–20]</sup> temperature,<sup>[20–22]</sup> electric pulse,<sup>[23–25]</sup>

light,<sup>[25]</sup> or the addition of guests.<sup>[26,27]</sup> To use light as an external trigger, a photoresponsive material is required. Of the organic photochromes, diarylethenes are very appealing due to the high thermal stability of both the open- and closed-ring isomers as well as their high fatigue resistance.<sup>[28–30]</sup>

We have previously reported a light-induced switching between two different 2D molecular orderings by isomerization of a diarylethene bearing pyrenyl group.<sup>[31]</sup> Herein we describe the properties of another diarylethene with three isomers (**1o**, **1c**, and **1a**, Figure 1) that form stable 2D molecular orderings on HOPG surface. A quantitative analysis of cooperativity in the formation of their 2D orderings and the mixing of components in the ordering will be discussed on the basis of the concentration dependence of the surface coverage of mono- and bicomponent systems.

## Results and Discussion

### Synthesis and photophysical properties

The diarylethene was designed to have long alkyl chains and amide groups for stabilization of the 2D ordering on HOPG.<sup>[32]</sup> The open-ring isomer **1o** was obtained by a two-step one-pot reaction starting from the corresponding bromo-substituted diarylethene in a yield of 94%. The closed-ring isomer **1c** was prepared by a classic photoreaction by irradiation of a solution of **1o** in ethyl acetate with UV light for 1 h. The isolated yield of compound **1c** was 72%. Irradiation of a solution of **1o** with UV light for 34 h afforded the annulated isomer **1a** in a yield of 17%.

The absorption spectra of the isolated three isomers were recorded in octanoic acid (OA) because this solvent was used in the STM measurements (Figure 2). The shapes and intensities of the absorption spectra were well reproduced by time-dependent density functional theory (TD-DFT) calculations at the B3LYP/6-311g(2d,p)//B3LYP/6-31g(d) level of theory (see Figures S1–S5 in the Supporting Information).

The ratio of the photoreaction quantum yields of diarylethene **1** for the cyclization ( $\Phi_{o \rightarrow c}$ ), cycloreversion ( $\Phi_{c \rightarrow o}$ ), and annulation reactions ( $\Phi_{c \rightarrow a}$ ) was estimated from the time evolution of the absorption spectra upon UV irradiation ( $\lambda_{\text{irrad}} = 365$  nm) in OA. Figure 3 shows the change in concentration

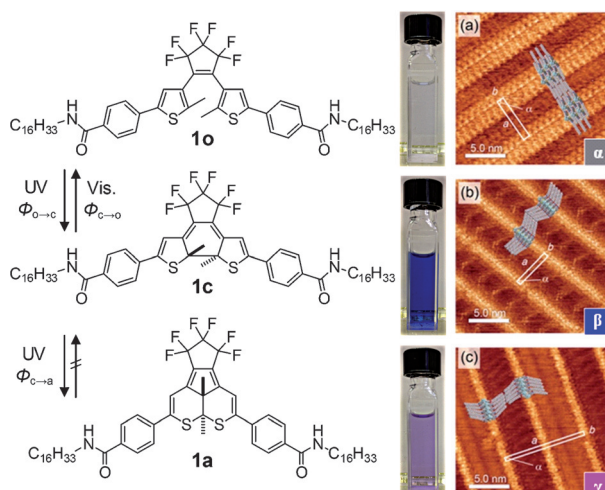


**Figure 1.** Chemical structures and STM images of (a) the open-ring isomer **1o** (ordering  $\alpha$ ), (b) the closed-ring isomer **1c** (ordering  $\beta$ ), and (c) the annulated isomer **1a** (ordering  $\gamma$ ). See ref. [32] for details of the orderings.

[a] Dr. D. Frath, Dr. T. Sakano, Y. Imaizumi, S. Yokoyama, Dr. T. Hirose, Prof. K. Matsuda

Department of Synthetic Chemistry and Biological Chemistry  
Graduate School of Engineering, Kyoto University  
Katsura, Nishikyo-ku, Kyoto 615-8510 (Japan)  
E-mail: kmatsuda@sbchem.kyoto-u.ac.jp

Supporting information for this article is available on the WWW under <http://dx.doi.org/10.1002/chem.201500804>.

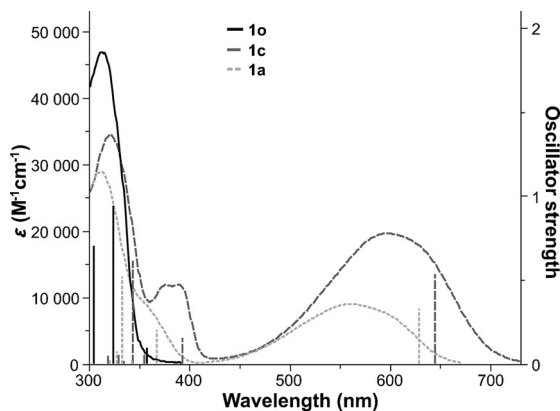


**Figure 2.** Absorption spectra of compounds **1o**, **1c**, and **1a** in octanoic acid and theoretical oscillator strengths calculated by TD-DFT.

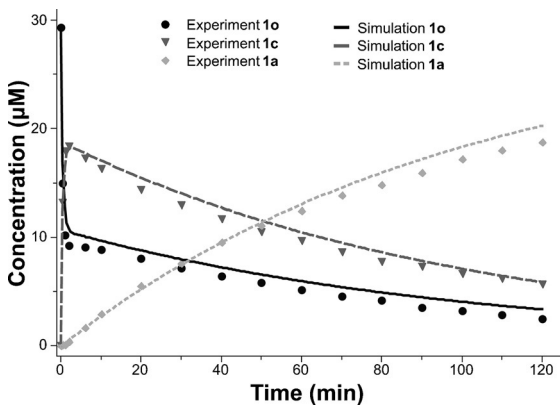


**Figure 3.** Evolution of the three isomers in octanoic acid upon UV irradiation ( $\lambda_{\text{irrad}} = 365 \text{ nm}$ ,  $[1\mathbf{o}]_{t=0} = 29.4 \mu\text{M}$ ,  $V = 3.0 \text{ mL}$ ,  $l = 1 \text{ cm}$ ).

with irradiation time, obtained by full-spectrum fitting of the time evolution of the absorption spectra shown in Figure S6 in the Supporting Information using the spectra of the three isomers shown in Figure 2. The differentiation of the concentration of each isomer is related to the reaction quantum yields ( $\Phi$ ) and molar absorption coefficients ( $\varepsilon$ ) according to Equations (1)–(3) in which  $\varepsilon_o$ ,  $\varepsilon_c$ , and  $\varepsilon_a$  are the molar absorption coefficients of each isomer at the irradiation wavelength,  $l$  is the optical path length,  $I_0$  is the intensity of irradiation, and  $A$  is given by Equation (4).

$$\frac{d[1\mathbf{o}]}{dt} = (\varepsilon_c[1\mathbf{c}]\phi_{c \rightarrow o} - \varepsilon_o[1\mathbf{o}]\phi_{o \rightarrow c}) \frac{(1 - 10^{-Al})I_0}{A} \quad (1)$$

$$\frac{d[1\mathbf{c}]}{dt} = (\varepsilon_o[1\mathbf{o}]\phi_{o \rightarrow c} - \varepsilon_c[1\mathbf{c}]\phi_{c \rightarrow o} - \varepsilon_c[1\mathbf{c}]\phi_{c \rightarrow a}) \frac{(1 - 10^{-Al})I_0}{A} \quad (2)$$

$$\frac{d[1\mathbf{a}]}{dt} = (\varepsilon_c[1\mathbf{c}]\phi_{c \rightarrow a}) \frac{(1 - 10^{-Al})I_0}{A} \quad (3)$$

$$A = \varepsilon_o[1\mathbf{o}] + \varepsilon_c[1\mathbf{c}] + \varepsilon_a[1\mathbf{a}] \quad (4)$$

To obtain a set of best-fit simulated curves, the ratio of the three reaction quantum yields was optimized by nonlinear re-

gression analysis of each step with the differential equations numerically solved simultaneously by using experimentally determined initial parameters. The resulting ratio  $\Phi_{o \rightarrow c}/\Phi_{c \rightarrow o}/\Phi_{c \rightarrow a}$  was 1:0.047:0.001. The photoreaction quantum yield for the annulation reaction ( $\Phi_{c \rightarrow a}$ ) was only 2.1% of the cycloreversion quantum yield ( $\Phi_{c \rightarrow o}$ ). Assuming that  $\Phi_{o \rightarrow c}$  is 0.59, as reported for a similar diarylethene derivative,<sup>[33]</sup> then  $\Phi_{c \rightarrow o}$  and  $\Phi_{c \rightarrow a}$  become  $2.8 \times 10^{-2}$  and  $6.0 \times 10^{-4}$ , respectively.

### Scanning tunneling microscopy

As reported previously, compounds **1o**, **1c**, and **1a** form characteristic stripe-patterned orderings ( $\alpha$ ,  $\beta$ , and  $\gamma$ , respectively) at the OA/HOPG interface (Figure 1).<sup>[32]</sup> It was also reported that only ordering  $\gamma$ , composed of compound **1a**, was observed after irradiation with UV light on the surface, even though the annulated isomer is only a photochemical byproduct generated with a small photogeneration yield, as mentioned above.<sup>[34]</sup> Ordering  $\beta$ , formed by the main photoproduct **1c**, was not observed after irradiating the surface with UV light.

To rationalize the reason for the favorable appearance of ordering  $\gamma$  upon in situ UV irradiation, we investigated the concentration dependence of the surface coverage by STM (Figure 4). Compound **1o** showed a gradual increase in the surface coverage with increasing concentration in the solution phase. The critical concentration, at which saturated adsorption was observed, was at around 30 μM for **1o**. The closed-ring isomer **1c** showed a sharp increase in the surface coverage with approximately the same critical concentration as the open-ring isomer (ca. 30 μM). The annulated isomer **1a** also showed a sharp increase in the surface coverage, but its critical concentration is at a lower concentration (ca. 15 μM). An interesting feature of compound **1a** is that the observed surface coverage was close to the theoretical maximum, which means that almost all molecules available in solution are involved in the construction of ordering  $\gamma$ . This suggests a very high affinity of **1a** for the HOPG surface.

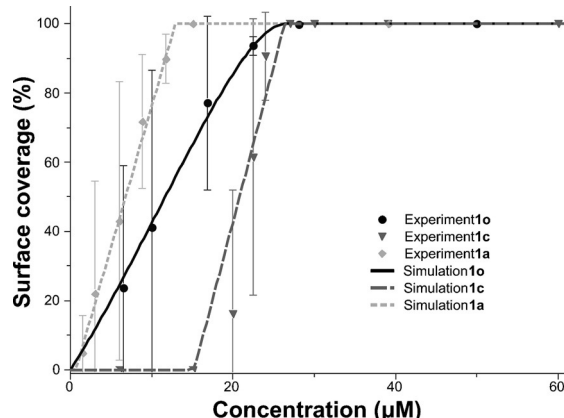


**Figure 4.** Concentration dependence of the surface coverage of **1o**, **1c**, and **1a** at the OA/HOPG interface. See the Supporting Information for STM images at different concentrations.

Once saturated adsorption at the interface was reached, an increase in concentration resulted in the formation of aggregates and/or multilayers on the surface for each of the isomers (see Figures S15, S24, and S31 in the Supporting Information). At concentrations below the critical concentration, the domain size of the ordered area on the HOPG is usually larger than the scan size of the STM (ca.  $200 \times 200 \text{ nm}^2$ ). Typically, part of a large domain was observed in some images, whereas no ordering was observed in others. This fact creates a large dispersion of surface coverage data and is inevitably associated with large error bars, even if more data are collected (Figure 4). The stripe-patterned orderings  $\alpha$ ,  $\beta$ , and  $\gamma$  were thermodynamically stable and no polymorph was observed in the range of concentrations used in this study.

### Adsorption parameters (monocomponent systems)

Although the critical concentrations for **1o** and **1c** are almost the same, the steepness of the concentration dependence is clearly different for the two isomers. Therefore the critical concentration alone is not sufficient to characterize the ordering process. Inspired by cooperative supramolecular polymerization in solution,<sup>[35,36]</sup> an equilibrium model at the liquid/solid interface has recently been developed by our group.<sup>[37]</sup> The model considers two different equilibrium constants, nucleation ( $K_n$ ) and elongation ( $K_e$ ) equilibrium constants, and so takes into account the intermolecular interactions between neighboring molecules on the substrate. It can be noted that the experimental concentration dependence of the surface coverage is well reproduced by using these two parameters (Figure 4).

According to this model, the fractional coverage  $\theta$  can be described by Equation (5) in which  $\sigma$  is the degree of cooperativity defined as the ratio  $K_n/K_e$ ,  $c_t$  is the total concentration of the component, and  $\alpha$  is defined by Equation (6) in which  $A_{\text{sub}}$  is the total area of the substrate,  $L$  is the volume of the supernatant solution,  $S$  is the surface area occupied by one molecule, and  $N_A$  is the Avogadro constant. Because the formation of molecular ordering at the liquid/solid interface is a 2D crystal growth process, it should comply with a cooperative model in which  $K_n$  is less than  $K_e$  ( $\sigma < 1$ ).

$$\theta = (1 - \theta) \frac{\sigma K_e (c_t - \alpha \theta)}{[1 - K_e (c_t - \alpha \theta)]^2} \quad (5)$$

$$\alpha = \frac{A_{\text{sub}}}{L N_A S} \quad (6)$$

The simulated curves that fit best the experimental data are shown in Figure 4 and the adsorption parameters are presented in Table 1. The experimental data for the open-ring isomer **1o** were sufficiently well reproduced by considering isodesmic adsorption in which the nucleation and subsequent elongation steps have almost identical equilibrium constants ( $K_n \approx K_e$ ,  $\sigma \approx 1$ ). The elongation constant of **1c** ( $K_e = 6.6 \times 10^4 \text{ M}^{-1}$ ) is comparable to that of **1o** ( $K_e = 6.8 \times 10^4 \text{ M}^{-1}$ ), whereas the nuclea-

**Table 1.** Best-fitting adsorption parameters for **1o**, **1c**, and **1a** at the OA/HOPG interface (monocomponent parameters).<sup>[a]</sup>

Compound	$K_e [\text{M}^{-1}]$	$K_n [\text{M}^{-1}]$	$\sigma$
<b>1o</b>	$6.8 \times 10^4$	$6.4 \times 10^4$	0.95
<b>1c</b>	$6.6 \times 10^4$	$\leq 6.6 \times 10^{-2}$	$\leq 10^{-6}$ <sup>[b]</sup>
<b>1a</b>	$1.5 \times 10^6$	$\leq 1.5$	$\leq 10^{-6}$ <sup>[b]</sup>

[a] Simulated by the cooperative model on a 2D surface (monocomponent systems). [b] For values below  $10^{-6}$ , the curves are no longer significantly dependent on  $\sigma$ . Therefore a value of  $\sigma$  less than  $10^{-6}$  cannot be determined precisely.

tion constant of **1c** ( $K_n \leq 6.6 \times 10^{-2} \text{ M}^{-1}$ ) is almost six orders of magnitude less than that of the open-ring isomer **1o** ( $K_n = 6.4 \times 10^4 \text{ M}^{-1}$ ). Thus, the steep rise in the concentration dependence for the closed-ring isomer **1c** can be explained by a highly cooperative process ( $\sigma \leq 10^{-6}$ ).

The cooperative simulation ( $K_e = 1.5 \times 10^6 \text{ M}^{-1}$ ,  $\sigma \leq 10^{-6}$ ) gave the best-fitting curve for the experimental data of **1a**, although the isodesmic simulation ( $K_e = 1.0 \times 10^6 \text{ M}^{-1}$ ,  $\sigma = 1$ ) also gave an acceptable fitting (see Figure S8 in the Supporting Information). This result tells us that the simulated curves become less dependent on the degree of cooperativity ( $\sigma$ ) when the surface coverage is close to the theoretical maximum. Thus, it was difficult to determine which process controls the formation of ordering  $\gamma$ . Because no major difference was observed between the isodesmic and cooperative curves for **1a**, the cooperative model was applied to the subsequent calculations.

The favorable appearance of ordering  $\gamma$  upon photoirradiation can be quantitatively explained by the large  $K_e$  value for **1a** ( $K_e \geq 10^6 \text{ M}^{-1}$ ), which is associated with the very high affinity of the annulated isomer for the HOPG surface. The elongation constant for the annulated isomer **1a** is even higher by almost two orders of magnitude than those of **1o** and **1c**. Our model, using two adsorption parameters ( $K_e$  and  $\sigma$ ), is a very convenient tool for the quantitative evaluation of the concentration dependence of ordering formation on a 2D surface. Moreover, the surface coverage  $\theta$  can be calculated at any concentration based on the two parameters.

### Preirradiation experiment

For a careful investigation of fractional surface coverage in a multicomponent system composed of different isomers, the concentration of each isomer in solution should be precisely determined. A solution of the open-ring isomer **1o** (28.7  $\mu\text{M}$ ) was irradiated with UV light ( $\lambda_{\text{irrad}} = 365 \text{ nm}$ ) for 5, 15, and 45 min and the concentration of each sample was determined by UV/Vis spectroscopy. STM images were then acquired for the three concentration-determined samples that were irradiated before deposition on the HOPG (Figure 5 and S32–S34 in the Supporting Information). The respective fractional coverages observed for orderings  $\alpha$ ,  $\beta$ , and  $\gamma$  are summarized in Table S1 in the Supporting Information.

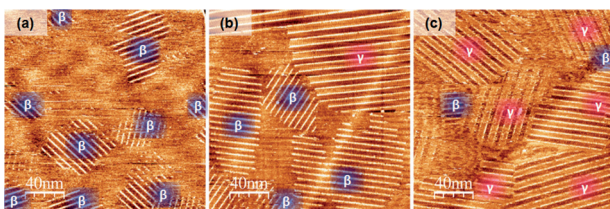


**Figure 5.** Representative STM images ( $200 \times 200 \text{ nm}^2$ ) obtained by the deposition of preirradiated solutions in OA ( $I_{\text{set}} = 10 \text{ pA}$ ,  $V_{\text{bias}} = -1.0 \text{ V}$ ,  $[1\text{o}]_0 = 28.7 \mu\text{M}$ ). UV irradiation ( $\lambda_{\text{irrad}} = 365 \text{ nm}$ ) was conducted for (a) 5, (b) 15, and (c) 45 min prior to deposition on HOPG. The concentration of each sample was precisely determined by UV/Vis spectroscopy (Table 3).

From the exact composition of the mixture, the fractional coverage  $\theta$  for each isomer can be calculated based on the adsorption parameters determined above. The experimentally observed fractional coverages of ordering  $\gamma$  ( $\theta_{\gamma,\text{exp}} = 0, 0.32$ , and  $0.79$ ) for the samples after UV irradiation for 5, 15, and 45 min, respectively, are quite similar to the simulated values ( $\theta_{\gamma,\text{sim}} = 0.09, 0.26$ , and  $0.87$ ), which suggests that the adsorption of **1a** can be reproduced with monocomponent parameters. However, the experimental coverages for **1o** and **1c** ( $\theta_{\alpha,\text{exp}} = 0$  for all samples;  $\theta_{\beta,\text{exp}} = 0.35, 0.18$ , and  $0.005$ ) were surprisingly different from expectation ( $\theta_{\alpha,\text{sim}} = 0.40, 0.32$ , and  $0.21$ ;  $\theta_{\beta,\text{sim}} = 0.08, 0.02$ , and  $0$ ); the experimental coverages for ordering  $\beta$  are significantly higher than the predictions and ordering  $\alpha$  was not observed experimentally. These observations suggest that the open- and closed-ring isomers significantly influence each other during the formation of their 2D orderings. As described in the next section, the experimental surface coverage was reproduced well by considering a mixing of the two isomers in the orderings  $\alpha$  and  $\beta$ .

#### Adsorption parameters (bicomponent systems)

To identify the interactions between the two isomers **1o** and **1c**, the concentration dependence of the surface coverage for the bicomponent system was carefully investigated (Figure 6). Interestingly, only ordering  $\beta$  was observed for **1o/1c** ratios of 0:100, 37:63, and 51:49 (Figure 6a), and ordering  $\alpha$  was solely observed for ratios of 78:22 and 100:0 (Figure 6b). Both orderings  $\alpha$  and  $\beta$  were observed simultaneously in the STM images of a narrow range of ratios such as 62:38.<sup>[32]</sup> The simultaneous observation of the two orderings is also possible by drop-casting a concentrated solution of **1c** onto a preadsorbed solution of **1o**.<sup>[32]</sup>

The effect of the presence of **1o** on the formation of ordering  $\beta$  is clearly seen in Figure 6a. We assumed that the ordering  $\beta$  consists of only the closed-ring isomer and the surface coverage of ordering  $\beta$  is plotted against the concentration of **1c**. If the formation of ordering  $\beta$  is independent of the presence of the open-ring isomer **1o**, the same concentration dependence is expected for any ratio of isomers **1o/1c**. However, the critical concentration of **1c** is clearly reduced from 26 to 21  $\mu\text{M}$  with an increasing fraction of **1o**. At a given concentration of **1c**, the surface coverage of ordering  $\beta$  is significantly increased by the addition of **1o**. For instance, pure **1c** at

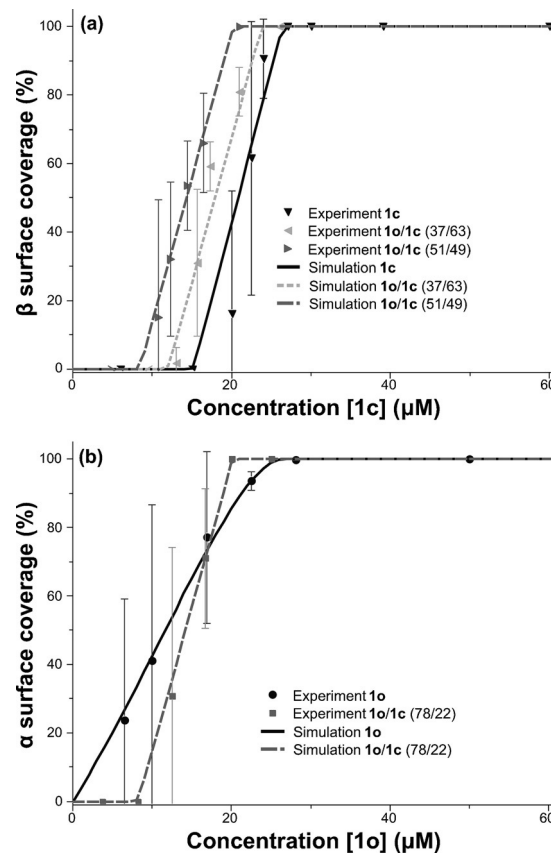


**Figure 6.** Concentration dependence of the surface coverage of (a) ordering  $\beta$  for **1c** and mixtures of **1o/1c** (37:63 and 51:49) and of (b) ordering  $\alpha$  for **1o** and a mixture of **1o/1c** (78:22). Simulated curves were obtained by using the adsorption parameters summarized in Table S2 in the Supporting Information.

15  $\mu\text{M}$  does not form any ordering whereas for samples with **1o/1c** ratios of 37:63 and 51:49 containing 15  $\mu\text{M}$  of **1c**, the surface coverage of ordering  $\beta$  reaches 25 and 56%, respectively. This significant increase in surface coverage upon addition of **1o** suggests that the ordering  $\beta$  is likely a mixed crystal composed of the two isomers.

Because mixing of two isomers in orderings  $\alpha$  and  $\beta$  was experimentally suggested, we assumed that the open- and closed-ring isomers cocrystallize on the 2D surface and that both **1o** and **1c** contribute equally to the formation of orderings  $\alpha$  and  $\beta$ . On the basis of this assumption, the experimental surface coverage was plotted against the total concentration of the two isomers  $[1\text{o} + 1\text{c}]$  (Figure 7). The resulting curves are shown in Figure 7 and the corresponding adsorption parameters are presented in Table 2.

Upon mixing the open-ring isomer **1o** in the ordering  $\beta$ , which mainly consists of the closed-ring isomer **1c**, the critical concentration increased from 26 to around 40  $\mu\text{M}$  for the **1o/1c** ratio of 51:49 (Figure 7a). This is associated with a decrease in the elongation equilibrium constant ( $K_e$ ) from  $6.6 \times 10^4$  to  $3.9 \times 10^4 \text{ M}^{-1}$  (Table 2). The decrease in  $K_e$  may be because of a thermodynamic destabilization of ordering  $\beta$  by the incorporation of the open-ring isomer **1o**, which has a slightly differ-

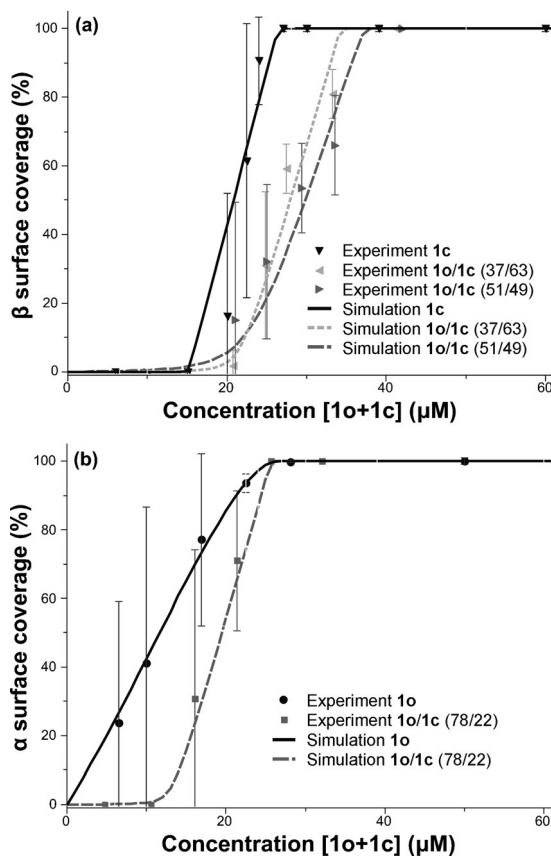


**Figure 7.** Concentration dependence of the surface coverage of (a) ordering  $\beta$  for **1c** and mixtures of **1o/1c** (37:63 and 51:49) and (b) ordering  $\alpha$  for **1o** and a mixture of **1o/1c** (78:22) against a total concentration of the two isomers [**1o + 1c**].

Table 2. Best-fitting adsorption parameters for solutions of <b>1o</b> and <b>1c</b> (bicomponent parameters). <sup>[a]</sup>					
Ratio <b>1o/1c</b>					
	0:100	37:63	51:49	78:22	100:0
Ordering	$\beta$	$\beta$	$\beta$	$\alpha$	$\alpha$
$K_e$ [ $M^{-1}$ ]	$6.6 \times 10^4$	$4.4 \times 10^4$	$3.9 \times 10^4$	$7.2 \times 10^4$	$6.8 \times 10^4$
$K_n$ [ $M^{-1}$ ]	$6.6 \times 10^{-2}$	$2.3 \times 10^1$	$1.9 \times 10^2$	$4.3 \times 10^1$	$6.4 \times 10^4$
$\sigma$	$\leq 10^{-6}$	$5.2 \times 10^{-4}$	$4.9 \times 10^{-3}$	$6.0 \times 10^{-4}$	0.95

[a] Simulated by using the cooperative model at a 2D surface.

Table 3. Experimental surface coverage for the preirradiation experiment and simulated values considering a mixing of <b>1o</b> and <b>1c</b> in the ordering $\alpha$ and $\beta$ . <sup>[a]</sup>										
Time [min] <sup>[b]</sup>	Concentration <sup>[c]</sup>			<b>1o/1c</b>	Surface coverage (experimental data) <sup>[d]</sup>			Surface coverage (simulated) <sup>[e]</sup>		
	[ <b>1o</b> ] [ $\mu M$ ]	[ <b>1c</b> ] [ $\mu M$ ]	[ <b>1a</b> ] [ $\mu M$ ]		$\theta_{\alpha,\text{exp}}$	$\theta_{\beta,\text{exp}}$	$\theta_{\gamma,\text{exp}}$	$\theta_{\alpha,\text{sim}}^{[f]}$	$\theta_{\beta,\text{sim}}^{[g]}$	$\theta_{\gamma,\text{sim}}^{[h]}$
5	9.4	16.1	1.8	37:63	0	0.35	0	0	0.31	0.09
15	7.8	14.9	3.9	34:66	0	0.18	0.32	0	0.14	0.26
45	5.1	9.5	11.3	35:65	0	0.005	0.79	0	0.003	0.87

[a] Corresponding STM images are shown in Figure 5 and S32–S34 in the Supporting Information. [b] Time of irradiation with UV light ( $\lambda_{\text{irrad}} = 365$  nm). [c] The concentrations of samples were determined by UV/Vis spectroscopy before deposition on the HOPG surface. [d] Experimental fractional surface coverage observed by STM measurements. [e] Simulated with the cooperative model using the adsorption parameters based on the total concentration of the two isomers [**1o + 1c**] (see Table 2). [f] No ordering was experimentally observed in the condition of the ratio of the two isomers **1o/1c**. [g] Values obtained by using bicomponent parameters ( $K_e = 4.4 \times 10^4 M^{-1}$ ,  $\sigma = 5 \times 10^{-4}$ ). [h] Values obtained by using monocomponent parameters ( $K_e = 1.5 \times 10^6 M^{-1}$ ,  $\sigma = 10^{-6}$ ).

ent conformation to **1c**. Upon the mixing of **1o** in ordering  $\beta$ , a significant decrease in cooperativity (i.e., increase in  $\sigma$  from less than  $10^{-6}$  to  $4.9 \times 10^{-3}$ ) was also observed, which originates from the increase in the nucleation equilibrium constant ( $K_n$ ) from  $6.6 \times 10^{-2}$  to  $1.9 \times 10^2 M^{-1}$ . Because the open-ring isomer **1o** has a higher nucleation equilibrium for the formation of ordering  $\alpha$  ( $K_n = 6.4 \times 10^4 M^{-1}$ ), it would act as a seeding agent giving a nucleation point for subsequent elongation of ordering  $\beta$ .

Upon mixing the closed-ring isomer **1c** in ordering  $\alpha$ , which is mainly composed of the open-ring isomer **1o**, a steep rise occurred in the concentration dependence of the surface coverage (Figure 7b). A prominent increase in the cooperativity (i.e.,  $\sigma$  decreased from 0.95 to  $6.0 \times 10^{-4}$ ) was observed in the adsorption parameters (Table 2). Thus, mixing-induced cooperativity in the formation of ordering  $\alpha$  is suggested.

The experimental surface coverage for the preirradiation experiment, shown in Figure 5, was re-analyzed by considering the mixing of the open- and closed-ring isomers in the orderings  $\alpha$  and  $\beta$ . In this analysis, the adsorption parameters for the ratio 37:63 ( $K_e = 4.4 \times 10^4 M^{-1}$ ,  $\sigma = 5.2 \times 10^{-4}$ ) were adopted because the experimental ratio is close to this value (i.e.,  $\mathbf{1o/1c} = (35.4 \pm 1.3)/(46.4 \pm 1.3)$  for the samples irradiated for 5, 15, and 45 min). As shown in Table 3, the experimental surface coverage was successfully reproduced by the simulation. In this context, the cocrystallization of the open- and closed-ring isomers in ordering  $\beta$  is further supported by the simulation considering the total concentration [**1o + 1c**].

Although we carefully took high-resolution STM images of the cocrystallized orderings, no significant difference has been observed at this time between ordering  $\alpha$  obtained from a pure solution of **1o** (Figure 8a) and from a mixed solution **1o/1c** (Figure 8b). The same is true for ordering  $\beta$  obtained from a pure solution of **1c** (Figure 8c) and from a mixed solution **1o/1c** (Figure 8d). Owing to a rapid exchange of components during the adsorption/desorption equilibrium at the OA/HOPG interface, a clear distinction between the two isomers at single-molecule resolution may be difficult under ambient conditions.

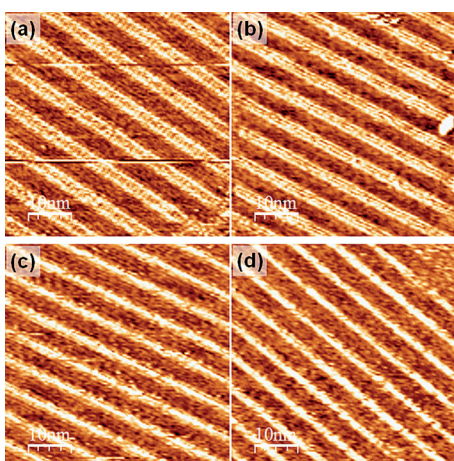


**Figure 8.** High-resolution STM images ( $50 \times 50 \text{ nm}^2$ ,  $I_{\text{set}} = 10 \text{ pA}$ ,  $V_{\text{bias}} = -1.0 \text{ V}$ ) of (a) ordering  $\alpha$  for pure  $1\text{o}$  ( $[1\text{o}] = 16.9 \mu\text{m}$ ) and (b) for the sample with  $1\text{o}/1\text{c} = 78:22$  ( $[1\text{o} + 1\text{c}] = 16.1 \mu\text{m}$ ) and (c) ordering  $\beta$  for pure  $1\text{c}$  ( $[1\text{c}] = 24 \mu\text{m}$ ) and (d) for the sample with  $1\text{o}/1\text{c} = 37:63$  ( $[1\text{o} + 1\text{c}] = 27 \mu\text{m}$ ).

### Real-time *in situ* irradiation

Next, photochemical interchanges between orderings upon *in situ* photoirradiation were directly monitored by real-time STM scanning (Figure 9). Contrary to our expectation, the observed interchanges between orderings were different to those observed in the preirradiation experiment shown in Figure 5. STM images were continuously acquired at almost the same position on the substrate for 2 h (cf. the cross marked on Figure 9). After observation of the first STM image of the open-ring isomer  $1\text{o}$  ( $t = 0 \text{ min}$ ), the surface was constantly irradiated with UV light (365 nm) without stopping the STM scans. In the

initial image, several domains of ordering  $\alpha$  were observed. Upon UV irradiation, the surface coverage of ordering  $\alpha$  gradually decreased (12 min) until it had completely disappeared (59 min). In the meantime, several small domains of ordering  $\gamma$ , composed of the annulated isomer  $1\text{a}$ , appeared (14 min). These domains increased similar to a crystal growth (28 min) and eventually predominantly covered the substrate (38 min to 1 h 21 min).

According to the simulated evolution of concentrations (Figures 3 and S7 in the Supporting Information), the closed-ring isomer  $1\text{c}$  was expected to be predominant in the early stages of irradiation. However, ordering  $\beta$  was never observed during the course of the *in situ* irradiation. The favorable appearance of ordering  $\gamma$  upon UV irradiation of the surface is consistent with the previously reported result.<sup>[32]</sup> In the preirradiation experiment (Figure 5), the isomers with different ratios of  $1\text{o}/1\text{c}$  can start to adsorb onto an empty surface. On the other hand, in the *in situ* irradiation experiment (Figure 9), the surface is already almost fully occupied by ordering  $\alpha$ . We suppose that the closed-ring isomer  $1\text{c}$ , produced during the *in situ* irradiation, was progressively included in the preorganized ordering  $\alpha$ . Therefore the kinetically metastable ordering  $\alpha$ , composed of the two isomers  $1\text{o}$  and  $1\text{c}$ , was constantly observed until it was replaced by the more stable ordering  $\gamma$  having a higher affinity for the HOPG surface.

### Conclusions

In this work, the concentration dependence of surface coverage and photochemical interchanges between molecular orderings for the three isomers of a diarylethene were carefully investigated by UV/Vis spectroscopy and STM measurements. Adsorption parameters were determined by using a cooperative equilibrium model at a 2D surface for pure  $1\text{o}$ ,  $1\text{c}$ , and  $1\text{a}$ . According to these monocomponent parameters, the open-ring isomer  $1\text{o}$  showed an isodesmic process ( $\sigma \approx 1$ ) whereas the closed-ring isomer  $1\text{c}$  showed a highly cooperative process ( $\sigma \leq 10^{-6}$ ). The annulated isomer  $1\text{a}$  showed a very high affinity for the HOPG surface ( $K_e \geq 10^6$ ). Careful inspection of the bicomponent system of  $1\text{o}$  and  $1\text{c}$  suggested that the two isomers influence each other during the formation of molecular orderings and form mixed crystals. Moreover, mixing-induced cooperativity in the formation of ordering was observed by STM measurements: the closed-ring isomer  $1\text{c}$  can induce cooperativity into the formation of ordering  $\alpha$ , which is mainly composed of the open-ring isomer  $1\text{o}$ . The results presented in this work provide a better understanding of the mixing of components in molecular ordering and the photoinduced interchanges between orderings occurring at a liquid/solid interface.

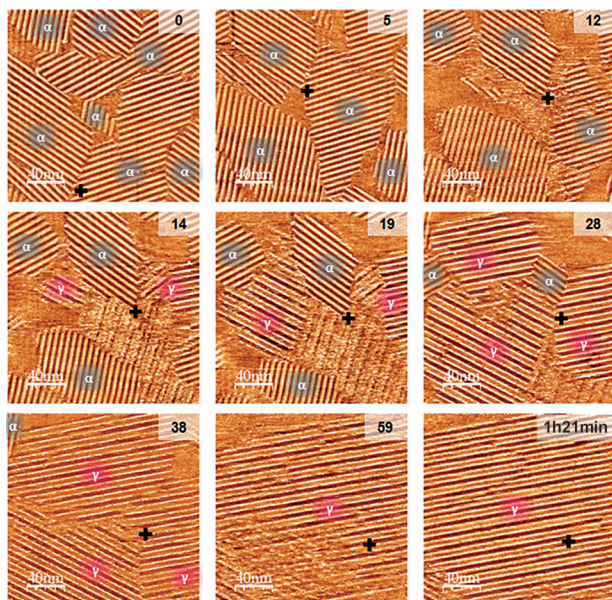


**Figure 9.** STM images ( $200 \times 200 \text{ nm}^2$ ) of the *in situ* photoirradiation of  $1\text{o}$  at the OA/HOPG interface ( $I_{\text{set}} = 10 \text{ pA}$ ,  $V_{\text{bias}} = -1.0 \text{ V}$ ,  $[1\text{o}]_{t=0} \sim 30 \mu\text{m}$ ). Times are given in minutes.

### Experimental Section

#### 1. Materials

**General methods:** Reagents and solvents were obtained from commercial suppliers and used without further purification. 1,2-Bis(2-methyl-5-bromo-3-thienyl)hexafluorocyclopentene and *N*-

hexadecyl-4-iodobenzamide were prepared according to methods reported in the literature.<sup>[32,38]</sup> All reactions were monitored by TLC carried out on 0.2 mm Merck silica gel plates (60F-254). Column chromatography was performed on silica gel (Nakalai Tesque, 70–230 mesh). <sup>1</sup>H and <sup>13</sup>C NMR spectra were recorded on a JEOL JNM-ALPHA500 or JNM-ECA600 spectrometer. Proton chemical shifts are reported in ppm downfield from tetramethylsilane (TMS). Carbon chemical shifts are reported in ppm by reference to the solvent signal. Mass spectra were recorded with a Thermo Scientific Exactive ESI-Orbitrap mass spectrometer.

**Synthesis of the open-ring isomer 1o:** *n*BuLi (1.6 M in hexane, 0.60 mL, 0.96 mmol) was added to a solution of 1,2-bis(2-methyl-5-bromo-3-thienyl)hexafluorocyclopentene (200 mg, 0.380 mmol) in dry THF (15 mL) at –78 °C under a nitrogen atmosphere. The resulting mixture was stirred for 1 h at –78 °C. Then tributyl borate (0.30 mL, 1.1 mmol) was added. The solution was warmed to room temperature and stirred for 3 h. Then *N*-hexadecyl-4-iodobenzamide (358 mg, 0.759 mmol) and aq. K<sub>2</sub>CO<sub>3</sub> (20 wt %, 15 mL) were added. After bubbling argon through the solution, [Pd(PPh<sub>3</sub>)<sub>4</sub>] was added and the solution was heated at reflux for 16 h under an argon atmosphere. After cooling, the mixture was washed with aq. NH<sub>4</sub>Cl and extracted with diethyl ether. Organic layers were collected, dried over MgSO<sub>4</sub>, filtered, and concentrated under vacuum. The residue was purified by silica gel chromatography eluting with chloroform to give a white-blue powder. Yield: 94% (378 mg); <sup>1</sup>H NMR (500 MHz, CDCl<sub>3</sub>): δ = 7.71 (d, *J* = 8.6 Hz, 2H), 7.58 (d, *J* = 8.6 Hz, 2H), 7.34 (s, 2H), 6.13–6.10 (m, 2H), 3.49–3.44 (m, 4H), 1.99 (s, 6H), 1.64–1.61 (m, 4H), 1.40–1.26 (m, 52H), 0.88 ppm (t, *J* = 7.0 Hz, 6H); <sup>13</sup>C NMR (151 MHz, CDCl<sub>3</sub>): δ = 166.9, 142.5, 141.3, 136.2, 134.1, 127.9, 126.2, 125.7, 123.6, 40.4, 32.1, 29.89, 29.86, 29.80, 29.77, 29.57, 29.55, 27.2, 22.9, 14.8, 14.3 ppm; UV/Vis (octanoic acid): λ<sub>max</sub> (*ε*) = 311 nm (46 900 M<sup>−1</sup> cm<sup>−1</sup>); HRMS (ESI): *m/z* calcd for C<sub>61</sub>H<sub>84</sub>F<sub>6</sub>N<sub>2</sub>O<sub>2</sub>S<sub>2</sub>H<sup>+</sup>: 1055.5951 [M+H]<sup>+</sup>; found: 1055.5948.

**Synthesis of the closed-ring isomer 1c:** A solution of 1o (20 mg) in ethyl acetate (200 mL) was irradiated with a UV light (*λ* = 313 nm) for 1 h. Compound 1c was purified by HPLC (Mightysil Si60 250–20, eluting with dichloromethane/EtOAc 90:10, 5.0 mL min<sup>−1</sup>, retention time 19 min) to give a blue solid. Yield: 72% (14.4 mg); <sup>1</sup>H NMR (500 MHz, CDCl<sub>3</sub>): δ = 7.80 (d, *J* = 8.6 Hz, 4H), 7.61 (d, *J* = 8.6 Hz, 4H), 6.73 (s, 2H), 6.20–6.16 (m, 2H), 3.49–3.45 (m, 4H), 2.20 (s, 6H), 1.68–1.61 (m, 4H), 1.39–1.26 (m, 52H), 0.88 ppm (t, *J* = 7.0 Hz, 6H); <sup>13</sup>C NMR (151 MHz, CDCl<sub>3</sub>): δ = 166.5, 157.0, 149.5, 136.5, 135.7, 127.6, 127.2, 115.3, 66.4, 40.5, 32.2, 29.92, 29.88, 29.82, 29.77, 29.6, 29.5, 27.2, 25.5, 22.9, 14.3 ppm; UV/Vis (octanoic acid): λ<sub>max</sub> (*ε*) = 598 (19 700), 390 (12 000), 377 (12 000), 320 (34 500 M<sup>−1</sup> cm<sup>−1</sup>); HRMS (ESI): *m/z* calcd for C<sub>61</sub>H<sub>84</sub>F<sub>6</sub>N<sub>2</sub>O<sub>2</sub>S<sub>2</sub>H<sup>+</sup>: 1055.5951 [M+H]<sup>+</sup>; found: 1055.5940.

**Synthesis of the annulated isomer 1a:** A solution of 1o (20 mg) in ethyl acetate (200 mL) was irradiated with UV light (*λ* = 313 and 365 nm) for 34 h (2 × 17 h). Then it was irradiated with visible light (*λ* > 480 nm) for 17 h. A first purification by HPLC (Mightysil Si60 250–20, eluting with dichloromethane/EtOAc 90:10, 5.0 mL min<sup>−1</sup>) was used to remove most of the undesired isomers. Irradiation with visible light (*λ* > 480 nm) was repeated for 17 h. Compound 1a was purified by HPLC (Mightysil Si60 250–20, eluting with dichloromethane/EtOAc 90:10, 5.0 mL min<sup>−1</sup>, retention time 19.5 min) to give a deep-purple solid. Yield: 17% (3.4 mg); <sup>1</sup>H NMR (500 MHz, CDCl<sub>3</sub>): δ = 7.76 (d, *J* = 8.6 Hz, 2H), 7.59 (d, *J* = 8.6 Hz, 2H), 6.57 (s, 2H), 6.10–6.07 (m, 2H), 3.47–3.44 (m, 4H), 2.80 (s, 3H), 2.77 (s, 3H), 1.64–1.60 (m, 4H), 1.39–1.24 (m, 52H), 0.88 ppm (t, *J* = 7.0 Hz, 6H); <sup>13</sup>C NMR: Not obtained due to the limited amount of compound; UV/Vis (octanoic acid) λ<sub>max</sub> (*ε*) = 560 (9100), 313 (29 100 M<sup>−1</sup> cm<sup>−1</sup>);

HRMS (ESI): *m/z* calcd for C<sub>61</sub>H<sub>84</sub>F<sub>6</sub>N<sub>2</sub>O<sub>2</sub>S<sub>2</sub>H<sup>+</sup>: 1055.5951 [M+H]<sup>+</sup>; found: 1055.5936.

## 2. Theoretical calculations

The geometrical optimization was carried out at the RB3LYP/6-31g(d) level of theory. Convergence to a local minimum structure was confirmed by no imaginary frequencies on frequency analysis. The optimized local minimum structures were successively subjected to TD-DFT calculations to obtain 10 excited states from the lowest-energy transition at the identical level of theory.

## 3. UV/Vis spectroscopy and photochemical reactions

Absorption spectra were recorded with a HITACHI U-3310 spectrophotometer using quartz cells with an optical length of 1 cm. Photoirradiation experiments on the HOPG surface were performed by using a Keyence UV-400 UV-LED equipped with an optical fiber (0.30 W cm<sup>−2</sup>, *λ* = 365 nm) or a USHIO 500 W xenon lamp with a UV-29 sharp cut filter and U340 bandpass filter for UV light (0.64 W cm<sup>−2</sup>, *λ*<sub>max</sub> = 313 nm), and with UV-29 and Y-48 sharp cut filters for visible light (0.32 W cm<sup>−2</sup>, *λ* > 460 nm).

## 4. Scanning tunneling microscopy

All STM experiments were performed at room temperature under ambient conditions. The STM images were acquired with an Agilent technologies 5500 scanning probe microscope in constant current mode. The STM tips were mechanically cut from a Pt/Ir (80:20, diameter 0.25 mm) wire. Highly oriented pyrolytic graphite (HOPG, purchased from the Bruker Co.) was used as substrate. The concentrations of solutions were controlled by UV/Vis analysis. A drop of the solution (8 μL) was deposited onto freshly cleaved HOPG, the tip was immersed into the solution, and images were scanned. Topography images were obtained by using the WSxM software.<sup>[39]</sup>

## Acknowledgements

This work was supported by the NEXT program (No. GR062), a Grant-in-Aid for Scientific Research on Innovative Areas “photosynergetics” (No. 26107008) from MEXT, a Grant-in-Aid for Young Scientists (B) (No. 25810048), and a Grant-in-Aid for JSPS Fellows (No. 2604341) from the Japan Society for the Promotion of Science (JSPS). D.F. acknowledges the JSPS for a post-doctoral fellowship.

**Keywords:** cooperative effects • mixed crystals • photochromism • scanning tunneling microscopy • self-assembly

- [1] J. V. Barth, G. Costantini, K. Kern, *Nature* **2005**, *437*, 671–679.
- [2] T. Kudernac, S. Lei, J. A. A. W. Elemans, S. De Feyter, *Chem. Soc. Rev.* **2009**, *38*, 402–421.
- [3] K. S. Mali, J. Adisoefoso, E. Ghijssens, I. De Cat, S. De Feyter, *Acc. Chem. Res.* **2012**, *45*, 1309–1320.
- [4] A. G. Slater, P. H. Beton, N. R. Champness, *Chem. Sci.* **2011**, *2*, 1440–1448.
- [5] A. G. Slater, L. M. A. Perdigão, P. H. Beton, N. R. Champness, *Acc. Chem. Res.* **2014**, *47*, 3417–3427.
- [6] L. Piot, A. Marchenko, J. Wu, K. Müllen, D. Fichou, *J. Am. Chem. Soc.* **2005**, *127*, 16245–16250.
- [7] J. Adisoefoso, K. Tahara, S. Okuhata, S. Lei, Y. Tobe, S. De Feyter, *Angew. Chem. Int. Ed.* **2009**, *48*, 7353–7357; *Angew. Chem.* **2009**, *121*, 7489–7493.
- [8] K. Tahara, H. Yamaga, E. Ghijssens, K. Inukai, J. Adisoefoso, M. O. Blunt, S. De Feyter, Y. Tobe, *Nat. Chem.* **2011**, *3*, 714–719.

- [9] A. Ciesielski, M. El Garah, S. Haar, P. Kovaříček, J.-M. Lehn, P. Samori, *Nat. Chem.* **2014**, *6*, 1017–1023.
- [10] A. G. Slater, Y. Hu, L. Yang, S. P. Argent, W. Lewis, M. O. Blunt, N. R. Champness, *Chem. Sci.* **2015**, *6*, 1562–1569.
- [11] K. Cui, F. Schlüter, O. Ivasenko, M. Kivala, M. G. Schwab, S.-L. Lee, S. F. L. Mertens, K. Tahara, Y. Tobe, K. Müllen, *Chem. Eur. J.* **2015**, *21*, 1652–1659.
- [12] Arramel, T. C. Pijper, T. Kudernac, N. Katsonis, M. van der Maas, B. L. Ferlinga, B. J. van Wees, *Nanoscale* **2013**, *5*, 9277–9282.
- [13] S. V. Snegir, A. A. Marchenko, P. Yu, F. Maurel, O. L. Kapitanchuk, S. Mazerat, M. Lepeltier, A. Léautic, E. Lacaze, *J. Phys. Chem. Lett.* **2011**, *2*, 2433–2436.
- [14] B. Baisch, D. Raffa, U. Jung, O. M. Magnussen, C. Nicolas, J. Lacour, J. Kubitschke, R. Herges, *J. Am. Chem. Soc.* **2009**, *131*, 442–443.
- [15] C. Dri, M. V. Peters, J. Schwarz, S. Hecht, L. Grill, *Nat. Nanotechnol.* **2008**, *3*, 649–653.
- [16] L.-P. Xu, L.-J. Wan, *J. Phys. Chem. B* **2006**, *110*, 3185–3188.
- [17] S. De Feyter, F. C. De Schryver, *Chem. Soc. Rev.* **2003**, *32*, 139–150.
- [18] S. Lei, K. Tahara, F. C. De Schryver, M. Van der Auweraer, Y. Tobe, S. De Feyter, *Angew. Chem. Int. Ed.* **2008**, *47*, 2964–2968; *Angew. Chem.* **2008**, *120*, 3006–3010.
- [19] A. Ciesielski, P. J. Szabelski, W. Rżysko, A. Cadeddu, T. R. Cook, P. J. Stang, P. Samori, *J. Am. Chem. Soc.* **2013**, *135*, 6942–6950.
- [20] R. Gutzler, T. Sirtl, J. F. Dienstmaier, K. Mahata, W. M. Heckl, M. Schmittel, M. Lackinger, *J. Am. Chem. Soc.* **2010**, *132*, 5084–5090.
- [21] M. O. Blunt, J. Adisojoso, K. Tahara, K. Katayama, M. Van der Auweraer, Y. Tobe, S. De Feyter, *J. Am. Chem. Soc.* **2013**, *135*, 12068–12075.
- [22] D. Rohde, C.-J. Yan, H.-J. Yan, L.-J. Wan, *Angew. Chem. Int. Ed.* **2006**, *45*, 3996–4000; *Angew. Chem.* **2006**, *118*, 4100–4104.
- [23] Y. Okawa, M. Aono, *Nature* **2001**, *409*, 683–684.
- [24] M. Li, D. den Boer, P. Iavicoli, J. Adisojoso, H. Uji-i, M. Van der Auweraer, D. B. Amabilino, J. A. A. W. Elemans, S. De Feyter, *J. Am. Chem. Soc.* **2014**, *136*, 17418–17421.
- [25] A. Miura, S. De Feyter, M. M. S. Abdel-Mottaleb, A. Gesquière, P. C. M. Grim, G. Moessner, M. Sieffert, M. Klapper, K. Müllen, F. C. De Schryver, *Langmuir* **2003**, *19*, 6474–6482.
- [26] M. Blunt, X. Lin, M. del C. Gimenez-Lopez, M. Schroder, N. R. Champness, P. H. Beton, *Chem. Commun.* **2008**, 2304–2306.
- [27] S. Furukawa, K. Tahara, F. C. De Schryver, M. Van der Auweraer, Y. Tobe, S. De Feyter, *Angew. Chem. Int. Ed.* **2007**, *46*, 2831–2834; *Angew. Chem.* **2007**, *119*, 2889–2892.
- [28] M. Irie, *Chem. Rev.* **2000**, *100*, 1685–1716.
- [29] K. Matsuda, M. Irie, *J. Photochem. Photobiol. C* **2004**, *5*, 169–182.
- [30] M. Irie, T. Fukaminato, K. Matsuda, S. Kobatake, *Chem. Rev.* **2014**, *114*, 12174–12277.
- [31] R. Arai, S. Uemura, M. Irie, K. Matsuda, *J. Am. Chem. Soc.* **2008**, *130*, 9371–9379.
- [32] For preliminary work without cooperativity analysis, see: T. Sakano, Y. Imaizumi, T. Hirose, K. Matsuda, *Chem. Lett.* **2013**, *42*, 1537–1539.
- [33] M. Irie, T. Lifka, S. Kobatake, N. Kato, *J. Am. Chem. Soc.* **2000**, *122*, 4871–4876.
- [34] M. Irie, T. Lifka, K. Uchida, S. Kobatake, Y. Shindo, *Chem. Commun.* **1999**, 747–750.
- [35] D. Zhao, J. S. Moore, *Org. Biomol. Chem.* **2003**, *1*, 3471–3491.
- [36] T. F. A. De Greef, M. M. J. Smulders, M. Wolffs, A. P. H. J. Schenning, R. P. Sijbesma, E. W. Meijer, *Chem. Rev.* **2009**, *109*, 5687–5754.
- [37] S. Yokoyama, T. Hirose, K. Matsuda, *Chem. Commun.* **2014**, *50*, 5964–5966.
- [38] T. Saika, M. Irie, T. Shimidzu, *J. Chem. Soc. Chem. Commun.* **1994**, 2123–2124.
- [39] I. Horcas, R. Fernández, J. M. Gómez-Rodríguez, J. Colchero, J. Gómez-Herrero, A. M. Baro, *Rev. Sci. Instrum.* **2007**, *78*, 013705.

Received: February 27, 2015

Published online on June 26, 2015